Chin. Phys. Lett. **39**, 067404 (2022)

Pressure-Induced Superconductivity in Flat-Band Kagome Compounds $Pd_3P_2(S_{1-x}Se_x)_8$

Shuo Li(李硕)[1,2†], Shuo Han(韩烁)[2†], Shaohua Yan(闫少华)[2†], Yi Cui(崔祎)[2], Le Wang(王乐)[2], Shanmin Wang(王善民)[3], Shanshan Chen(陈珊珊)[2], Hechang Lei(雷和畅)[2*], Feng Yuan(袁峰)[4*], Jinshan Zhang(张金珊)[1*], and Weiqiang Yu(于伟强)[2*]

[1]*Mathematics and Physics Department, North China Electric Power University, Beijing 102206, China*
[2]*Department of Physics and Beijing Key Laboratory of Opto-electronic Functional Materials & Micro-nano Devices, Renmin University of China, Beijing 100872, China*
[3]*Department of Physics, Southern University of Science & Technology, Shenzhen 518055, China*
[4]*College of Physics, Qingdao University, Qingdao 266071, China*

(Received 29 March 2022; accepted 15 May 2022; published online 29 May 2022)

We performed high-pressure transport studies on the flat-band Kagome compounds, $Pd_3P_2(S_{1-x}Se_x)_8$ ($x = 0$, 0.25), with a diamond anvil cell. For both compounds, the resistivity exhibits an insulating behavior with pressure up to 17 GPa. With pressure above 20 GPa, a metallic behavior is observed at high temperatures in $Pd_3P_2S_8$, and superconductivity emerges at low temperatures. The onset temperature of superconducting transition T_C rises monotonically from 2 K to 4.8 K and does not saturate with pressure up to 43 GPa. For the Se-doped compound $Pd_3P_2(S_{0.75}Se_{0.25})_8$, the T_C is about 1.5 K higher than that of the undoped one over the whole pressure range, and reaches 6.4 K at 43 GPa. The upper critical field with field applied along the c axis at typical pressures is about 50% of the Pauli limit, suggesting a 3D superconductivity. The Hall coefficient in the metallic phase is low and exhibits a peaked behavior at about 30 K, which suggests either a multi-band electronic structure or an electron correlation effect in the system.

DOI: 10.1088/0256-307X/39/6/067404

Kagome lattice systems have been proposed to host rich physics, such as quantum spin liquid and unconventional superconductivity in systems with strong electron correlations.[1–5] Recently, the electronic flat band[6–15] and Dirac cones[9–11,16–22] were also observed and they caused intense research interests in several metallic kagome materials, where the electron correlations appear to be weak. In the Kagome lattice, the flat band arises from phase destruction of electron wave functions in the corner shared triangles, so that one electron band is localized in the hexagons.[23,24] Theoretically, the high electronic density of states in the flat band is expected to enhance the correlation effect if the flat band is close to the Fermi surface, which may give rise to unusual phenomena such as high T_C superconductivity,[2,25,26] fractional quantum Hall effect[27] and ferromagnetism.[28,29]

Unfortunately, the electron correlations in the flat-band Kagome materials seem to be too weak to offer any novel phase so far.[6–15] In parallel, signatures of flat bands and the related novel phases have been discovered experimentally in twisted bilayer graphene,[30,31] silicene[32] and dichalcogenides.[33] An alternative way to look for novel phases is to tune the materials by doping or pressure,[34,35] so that the electrons can be partly delocalized and bring in the electron correlation effect. In this regard, candidate Kagome materials having flat band close to Fermi surface, such as CoSn[9,10,36] and $Pd_3P_2S_8$,[14,15] are favored for further study by doping or pressure tuning.

In this Letter, we report our high-pressure transport studies on a van der Waals Kagome compound $Pd_3P_2S_8$ and its Se-doped compound $Pd_3P_2(S_{0.75}Se_{0.25})_8$, both of which are highly insulating at the ambient pressure.[14,15] Pd atoms in $Pd_3P_2S_8$ constitute the Kagome plane, as shown in Fig. 1. Local density approximation (LDA) calculations on $Pd_3P_2S_8$ reveal that a flat band, mainly formed by the d_{z^2} orbital of Pd^{2+}, is located at about 0.2 eV below the Fermi surface.[15] Se doping enhances the interlayer coupling and reduces the gap of the flat band.[15]

Our high-pressure transport studies show that for both compounds, the conductivity at 300 K is enhanced under pressure. At about 17 GPa, an insulating behavior is still seen. However, their conductivity exhibits a power-law temperature dependence in two decades of temperature below 300 K, which suggests strong electron localization caused by disorder.[37] With further increase of pressure above

†These authors contributed equally to this study.
*Corresponding authors. Email: hlei@ruc.edu.cn; yuan@qdu.edu.cn; zhangjs@ncepu.edu.cn; wqyu_phy@ruc.edu.cn
© 2022 Chinese Physical Society and IOP Publishing Ltd

20 GPa, a metallic behavior is induced at high temperatures. Superconductivity emerges at low temperatures in the metallic phase. The upper critical field is also found very high with field applied along the c axis. A small Hall coefficient is also observed in the metallic phase and exhibits a strong temperature dependence, which suggests that the system may have an electronic correlation effect.

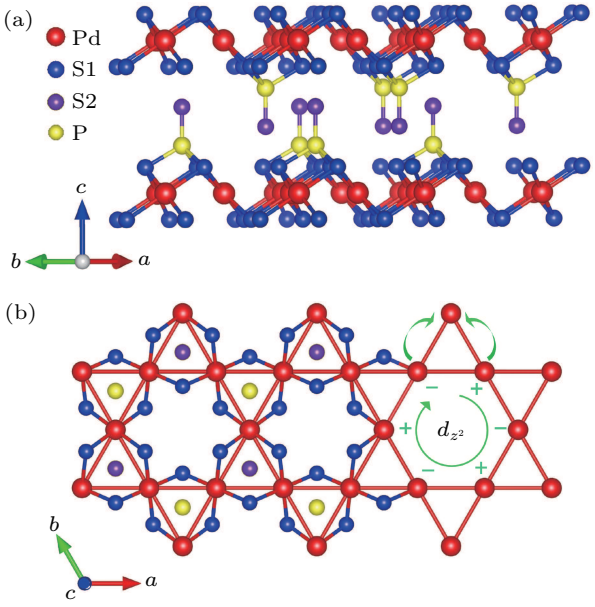

Fig. 1. (a) Planar view of the crystal structure of $Pd_3P_2S_8$. (b) Top view of one kagome layer. Phase destruction of the electron hopping is illustrated in a triangle, and electron localization is present in the hexagon. Here d_{z^2} labels the primary orbital that forms the flat band.

$Pd_3P_2(S_{1-x}Se_x)_8$ ($x = 0, 0.25$) single crystals were grown by the chemical vapor transport method.[14,15] As shown in Fig. 1(a), $Pd_3P_2S_8$ has a quasi-2D structure with S1–Pd–S1–P–S2 stacked sequentially along the c axis with an interlayer distance $c = 7.247$ Å,[15] and Pd atoms form a perfect kagome structure with the atomic distance $d_{\text{Pd-Pd}} = 3.418$ Å.[38] Doped Se replaces S atoms randomly and enhances the interlayer coupling,[15] which leads to a larger dispersion and a reduction of gap of the flat band. Note that $x = 0.25$ is the maximal Se doping level currently available.[15]

We performed high-pressure transport measurements with a BeCu diamond anvil cell (DAC). Diamond anvils of 300 μm culets and a rhenium gasket covered with cubic boron nitride (c-BN) powder were used, with no pressure transmitting medium filled in. The highest pressure we achieved is 43 GPa. The pressures were calibrated by the Raman spectrum from the culet of a top diamond anvil and fluorescence from the ruby using a Raman microscope (WITec Alpha 300R). For the transport measurements, the DAC, with sample loaded inside, is cooled in a Quantum Design physical property measurement system (PPMS-14T). The in-plane resistivity and the Hall resistivity of samples were performed by the standard van der Pauw method. Three single crystals, cut into dimensions of $100 \times 100 \times 15\ \mu m^3$, were measured. Two of them are undoped, labeled as S1 and S2 respectively, and one is doped, labeled as Se1.

The resistivity of three crystals is first measured with increasing pressures at zero field, and cooled from 300 K down to 2 K. Detailed data are shown as functions of temperatures in Figs. 2(a)–2(c). At ambient pressure, the resistance ρ of all three samples is large at room temperature and is barely measurable at low temperatures. This is consistent with the gapped behavior, where all the bands are away from the Fermi surface.[15] With applied pressure, the resistivity ρ decreases for all samples, as shown in Figs. 2(a)–2(c). For sample S1, the insulating behavior still holds under pressures of 17 and 21 GPa, as shown by the increase of resistivity upon cooling.

At 17 GPa, the conductivity of sample S1 is found to follow a power-law temperature dependence, that is, $\rho \sim 1/T^{\alpha}$ with the power-law exponent $\alpha = 0.801 \pm 0.001$, as shown by the fit in Fig. 2(a). The fitting holds in nearly two orders of temperature range below 300 K. By contrast, our data cannot be well fit to a gap function. This power-law temperature dependence of conductivity suggests that insulating behavior is caused by strong electron localization, as a result of disorder in the system.[37,39] In fact, it is found that $\alpha = 1$ for two-dimensional (2D) systems[40] and α ranges between 1/3 and 1/2 for 3D systems.[39,41] Our value of $\alpha \approx 0.8$ indicates that the system crossovers from the 2D to 3D at 17 GPa, which suggests that interlayer coupling is strongly enhanced under pressure. Note that the sample at the ambient pressure shows a high quality as revealed by our XRD data,[15] which leads us to speculate that the disorder effect is either an intrinsic pressure-induced structural disorder of the material, or brought in by pressure inhomogeneity under such high pressures.

A very weak upturn in resistivity is still observed at 21 GPa for sample S1, which suggests that the insulating behavior tends to be suppressed at pressures above 20 GPa. At and above 23 GPa, the resistivity decreases weakly upon cooling, which is a clear signature of a metallic behavior. An enlarged view of the low-temperature resistivity, at pressures above 20 GPa, is further demonstrated in the inset of Fig. 2(a). A high conductivity is seen with resistivity less than 0.5 mΩ·cm at room temperature. Since the resistivity does not show a large upturn upon cooling at low temperatures, a metallic, rather than an insulating behavior, is clearly established with pressure above 20 GPa.

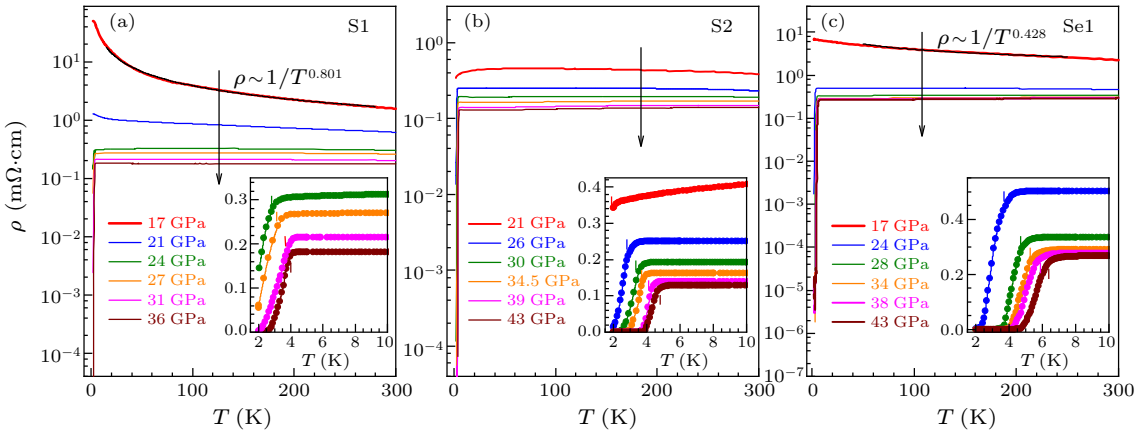

Fig. 2. (a) In-plane resistivity as functions of temperatures of undoped sample S1, measured under different pressures. The black solid line represents a power-law function fit, $\rho \sim 1/T^{0.801}$, to the data at 17 GPa. Inset: An enlarged view of low-temperature resistivity. (b)–(c) In-plane resistivity of undoped sample S2 and the Se-doped sample Se1, respectively, and an enlarged view of low-temperature resistivity in the inset. The black solid line in (c) is a function fit of $\rho \sim 1/T^{0.428}$ to the data at 17 GPa. Short vertical lines in the insets of (a)–(c) mark the 10% drop of the normal-state resistivity which signals the onset of superconductivity.

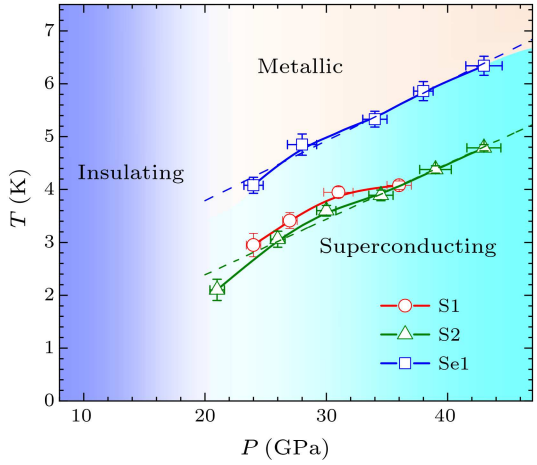

Fig. 3. The high-pressure phase diagram established on samples S1, S2, and Se1. The insulating (metallic) phase labels the regime where a prominent resistivity upturn is observed (absent) upon cooling. Open circles, triangles, and squares represent the onset T_C of the three samples, with the superconducting phase located below. The straight dashed lines are linear fit for the undoped and the Se-doped samples with the slope 0.105 K/GPa and 0.113 K/GPa, respectively.

Therefore, an insulating to metallic transition is revealed at about 20 GPa in sample S1. Similar transition is also observed for samples S2 and Se1, as shown in Figs. 2(b) and 2(c). Interestingly, the insulating to metallic transition for all the three samples occurs at pressures close to 20 GPa, as shown by the disappearance of the resistivity upturn in Figs. 2(b) and 2(c). For sample Se1, the conductivity at 17 GPa also follows the power-law fit with $\alpha \approx 0.428$ in a limited temperature range, as shown in Fig. 2(c). Such a lower α suggests that the doped sample has a strong 3D feature at the same pressure,[39,41] which is consistent with the LDA calculation that Se doping enhances interlayer coupling.[15]

When the metallic behavior is established at high temperatures, a sudden drop of resistivity for all the three samples is observed when further cooled, as shown in the insets of Figs. 2(a)–2(c). At even lower temperatures, zero resistivity is reached, which is clear evidence of superconductivity. The superconducting transition temperature, labeled as T_C, is defined by the temperature at which a 10% drop of normal-state resistivity is achieved, as shown in the inset of Figs. 2(a)–2(c). It is noticed that T_C rises continuously with pressure up to 43 GPa.

The T_C is then determined and plotted as functions of pressures for the three samples in the phase diagram in Fig. 3. Below 20 GPa, an insulating phase is established by the prominent resistivity upturn; whereas above 20 GPa, the absence of resistivity upturn reveals an onset of a metallic phase which turns into a superconductor at low temperatures. T_C rises monotonically with pressure for both the undoped and doped crystals. For the measured pressure range, T_C increases nearly linearly with pressure, at least up to 43 GPa. The slope is determined as $dT_C/dP = 0.11 \pm 0.05$ K/GPa for all the samples. At pressures above 30 GPa, a small increase in dT_C/dT is also observed, which suggests that a higher T_C should be achieved at pressures above 43 GPa.

It is also interesting to note that the T_C for the doped sample is about 1.5 K higher than the undoped one in the whole pressure range. In all compounds, superconductivity is not observed with pressure below 20 GPa, regardless of doping. This will be further discussed later.

Recently, two other studies[42,43] on $Pd_2P_2S_8$ also reported the pressure-induced superconductivity after this work, with T_C increasing monotonically with pressure. In Ref. [42], the onset pressure for super-

conductivity is about 10 GPa lower than ours, and T_C is about 2 K higher at the same pressures. In fact, a pressure-induced amorphous phase is found by the XRD and Raman scattering, which emerges simultaneously with superconductivity.[42,43] The difference of T_C may be caused by the pressure transmission medium used in different groups, since the amorphous phase should rely sensitively on the pressure conditions, as revealed by the strong hysteresis of superconductivity with pressure.[42]

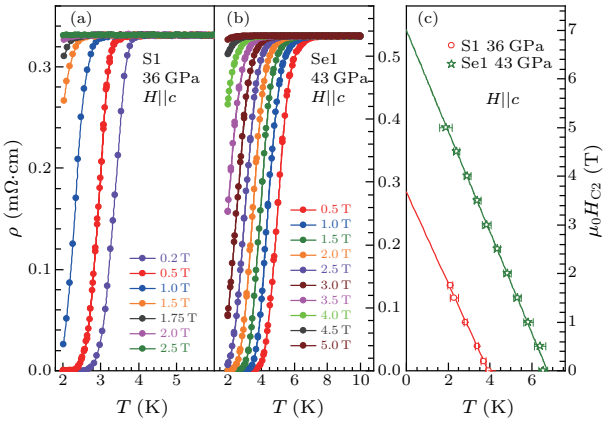

Fig. 4. [(a), (b)] Resistivity of samples S1 and Se1, as functions of temperatures measured with fields applied along the c axis, under pressure of 36 GPa and 43 GPa, respectively. (c) The out-of-plane H_{C2} of samples S1 and Se1 as functions of temperatures. The H_{C2} is defined by the magnetic field where the normal-state resistivity drops by 10% shown in (a) and (b). The solid lines in (c) are linear function fits of $H_{C2}(T)$ for samples S1 and Se1, respectively.

The out-of-plane upper critical field of superconductivity is also studied by the resistivity measurements with field applied along the crystalline c axis. The resistivity of samples S1 and Se1 are shown as functions of temperatures in Figs. 4(a) and 4(b) with different fields, each under a fixed pressure. For each fixed field, the resistivity of sample S1 measured at 36 GPa, as shown in Fig. 4(a), first rises from zero with increasing temperature. Above a specific temperature, resistivity exhibits a level off, which signals the disappearance of superconductivity; then the upper critical field H_{C2} at that temperature is determined as shown in Fig. 4(a). The H_{C2} of sample Se1 is also determined in the same way with data shown in Fig. 4(b), under a fixed pressure of 43 GPa.

The H_{C2} of both crystals is plotted as functions of temperatures in Fig. 4(c), which decreases with temperature. At low temperatures, H_{C2} drops almost linearly with field. Extrapolation to the zero temperature limit gives $H_{C2}(T=0) \approx 3.68$ T for sample S1, and $H_{C2}(0) \approx 7.0$ T for sample Se1. Considering the onset T_C at zero field to be about 4.08 K (6.4 K) for sample S1 (Se1), the zero temperature H_{C2} is then about 50% of the Pauli limit,[44–46] assuming $g = 2$. Such a high out-of-plane H_{C2} suggests that the system is likely a 3D superconductor, which is consistent with the resistivity measurements where a 2D to 3D crossover is already observed at 17 GPa as discussed above. Note that a high out-of-plane critical field is also reported in the iron-based superconductors.[47]

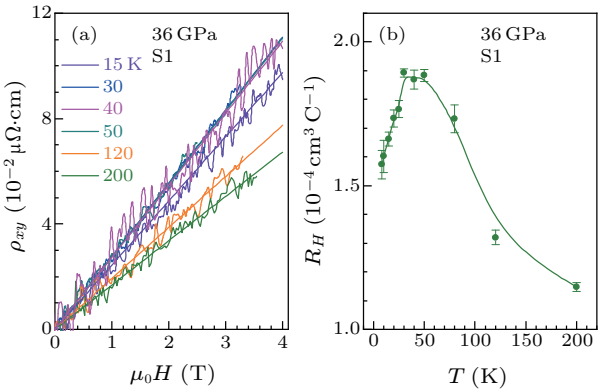

Fig. 5. (a) The in-plane Hall resistivity ρ_{xy} of sample S1 as functions of fields applied along the c axis, measured at different temperatures under a constant pressure 36 GPa. The straight lines are linear function fits to the data to calculate the Hall coefficient R_H. (b) The obtained R_H as a function of temperature.

To further understand the carrier properties, the Hall resistivity ρ_{xy} on sample S1 is measured with field applied along the c axis, under a pressure of 36 GPa. As shown in Fig. 5(a), ρ_{xy}, plotted as functions of fields measured at different temperatures, shows a linear field dependence with field up to 4 T. By taking the slope of the Hall resistivity, the Hall coefficient R_H is then calculated and plotted as a function of temperatures in Fig. 5(b). Both ρ_{xy} and R_H are calibrated by the high-pressure lattice parameters reported in Ref. [43]. R_H stays positive with temperatures from 200 K to 8 K, which suggests that the major carriers are the hole type in the system under pressure. However, R_H changes largely with temperature and is peaked at about 30 K. Such a dramatic temperature dependence suggests that the compounds either have multi electronic bands on the Fermi surface,[48,49] and/or have strong electron correlations.[49,50]

In fact, the values of R_H in the whole temperature range are very small, whose peaked value reads 1.89×10^{-4} cm^3/C at 30 K. Taking the value of R_H at 10 K, the carrier concentration is estimated to be 3.90×10^{22} cm^{-3} at this pressure, assuming a single band. However, this would suggest that each unit cell contains an excessive carrier density of 9.26 holes per unit cell at 10 K. To understand the small and temperature-dependent R_H, we propose two alternative scenarios as described below.

The first scenario is based on the nearly compensated electron and hole bands on the Fermi surface. If the system contains both hole and electron types of carriers at high pressures, the value of R_H

can be very small as observed. Together with the large temperature-dependent $R_{\rm H}$ as described above, a pressure induced multi-band system, with both electron and hole types of carriers on the Fermi surface, is suggested for the high pressure phase. Comparing with the band structure calculations,[15] the d_{z^2} band of Pd^{2+} is only slightly below the Fermi surface, which may constitute the hole band. By contrast, the $d_{x^2-y^2}$ orbital is located at about 1.5 eV above the Fermi surface, which may become the electron band at high pressures.

The second scenario is based on the correlation effect of the flat band. With more portion of the (nearly) flat band pushed to the Fermi surface under pressure, both the carrier density and the electron correlation effect may be strongly enhanced simultaneously, which result in the temperature-dependent Hall coefficient with a small value. Given the non-monotonic change of the Hall coefficient with temperature, the electron correlation scenario is favored.

To our knowledge, this is a rare superconductor derived from a Kagome compound with a flat band. We now attempt to understand the pressure and Se doping effect in all the samples. As reported, the emergence of superconductivity depends on the pressure-induced structural transition from the crystalline to amorphous phase.[42,43] The emergence of the amorphous phase is consistent with our resistivity data, where large disorder is already observed in the low-pressure phase by the power-law temperature dependence of conductivity. At pressures above 20 GPa, however, the large carrier density may mask the power-law behavior in the conductivity. In principle, further increase of pressure may push the flat band more dispersive, which results in higher carrier concentration on the Fermi surface and enhances $T_{\rm C}$ consequently. Se doping may also enhance $T_{\rm C}$ by the increase of the hoping elements with more extended orbitals of Se. On the other hand, the emergence of superconductivity relies only on the external pressure which causes the amorphous phase, so that superconductivity occurs at a similar pressure for both the parent and the doped compounds.

In summary, our high-pressure transport studies on the undoped and the Se-doped $Pd_3P_2S_8$ reveal that the resistivity changes from an insulating to a metallic behavior at about 20 GPa. The power-law temperature dependence of conductivity at low pressure suggests a high level of disorder induced by pressure, with a 2D to 3D crossover. Superconductivity is observed in the metallic phase for all the compounds. The out-of-plane $H_{\rm C2}$ is high, which again suggests a 3D nature of superconductivity. The superconducting transition temperature $T_{\rm C}$ rises with pressure at least up to 43 GPa. Here, 25% Se doping further enhances $T_{\rm C}$ by 1.5 K. Our data suggest that the high-pressure phase likely has both electron and hole bands on the Fermi surface, or strong electron correlations, as revealed by the small value of the Hall coefficient and its large, non-monotonic temperature dependence.

W.Y. and Y.C. are supported by the National Natural Science Foundation of China (Grant Nos. 51872328, 12134020, and 12104503), the National Key R&D Program of China (Grant No. 2016YFA0300504), the Fundamental Research Funds for the Central Universities and the Research Funds of Renmin University of China (Grant Nos. 21XNLG18 and 18XNLG24). Y.C. is also supported by the China Postdoctoral Science Foundation (Grant No. 2020M680797). H.C.L is supported by the National Key R&D Program of China (Grant No. 2018YFE0202600), the Beijing Natural Science Foundation (Grant No. Z200005), the Fundamental Research Funds for the Central Universities and the Research Funds of Renmin University of China (Grant Nos. 18XNLG14, 19XNLG13, and 19XNLG17).

References

[1] Anderson P W 1987 *Science* **235** 1196
[2] Ko W H, Lee P A and Wen X G 2009 *Phys. Rev. B* **79** 214502
[3] Han T H, Helton J S, Chu S Y, Nocera D G, Rodriguez-Rivera J A, Broholm C and Lee Y S 2012 *Nature* **492** 406
[4] Wen J S, Yu S L, Li S Y, Yu W Q and Li J X 2019 *npj Quantum Mater.* **4** 12
[5] Wei Y, Ma X Y, Feng Z L, Zhang Y C, Zhang L, Yang H X, Qi Y, Meng Z Y, Wang Y C, Shi Y G and Li S L 2021 *Chin. Phys. Lett.* **38** 097501
[6] Lin Z Y, Choi J H, Zhang Q, Qin W, Yi S, Wang P D, Li L, Wang Y F, Zhang H, Sun Z, Wei L M, Zhang S B, Guo T F, Lu Q Y, Cho J H, Zeng C G and Zhang Z Y 2018 *Phys. Rev. Lett.* **121** 096401
[7] Yin J X, Zhang S T, Chang G Q, Wang Q, Tsirkin S S, Guguchia Z, Lian B, Zhou H B, Jiang K, Belopolski I, Shumiya N, Multer D, Litskevich M, Cochran T A, Lin H, Wang Z Q, Neupert T, Jia S, Lei H C and Hasan M Z 2019 *Nat. Phys.* **15** 443
[8] Kang M G, Ye L D, Fang S A, You J S, Levitan A, Han M Y, Facio J I, Jozwiak C, Bostwick A, Rotenberg E, Chan M K, McDonald R D, Graf D, Kaznatcheev K, Vescovo E, Bell D C, Kaxiras E, van den Brink J, Richter M, Prasad G M, Checkelsky J G and Comin R 2020 *Nat. Mater.* **19** 163
[9] Kang M G, Fang S A, Ye L D, Po H C, Denlinger J, Jozwiak C, Bostwick A, Rotenberg E, Kaxiras E, Checkelsky J G and Comin R 2020 *Nat. Commun.* **11** 4004
[10] Liu Z H, Li M, Wang Q, Wang G W, Wen C H P, Jiang K, Lu X L, Yan S C, Huang Y B, Shen D W, Yin J X, Wang Z Q, Yin Z P, Lei H C and Wang S C 2020 *Nat. Commun.* **11** 4002
[11] Li M, Wang Q, Wang G W, Yuan Z H, Song W H, Lou R, Liu Z T, Huang Y B, Liu Z H, Lei H C, Yin Z P and Wang S C 2021 *Nat. Commun.* **12** 3129
[12] Han M Y, Inoue H, Fang S A, John C, Ye L D, Chan M K, Graf D, Suzuki T, Ghimire M P, Cho W J, Kaxiras E and Checkelsky J G 2021 *Nat. Commun.* **12** 5345
[13] Ye L D, Fang S A, Kang M G, Kaufmann J, Lee Y H, Denlinger J, Jozwiak C, Bostwick A, Rotenberg E, Kaxiras E, Bell D C, Janson O, Comin R and Checkelsky J G 2021

arXiv:2106.10824 [cond-mat.mtrl-sci]
[14] Park S, Kang S, Kim H, Lee K H, Kim P, Sim S, Lee N, Karuppannan B, Kim J, Kim J, Sim K I, Coak M J, Noda Y, Park C H, Kim J H and Park J G 2020 *Sci. Rep.* **10** 20998
[15] Yan S H, Gong B C, Wang L, Wu J Z, Yin Q W, Cao X Y, Zhang X, Liu X F, Lu Z Y, Liu K and Lei H C 2022 *Phys. Rev. B* **105** 155115
[16] Liu E K, Sun Y, Kumar N, Muechler L, Sun A L, Jiao L, Yang S Y, Liu D F, Liang A J, Xu Q N, Kroder J, Süß V, Borrmann H, Shekhar C, Wang Z S, Xi C Y, Wang W H, Schnelle W, Wirth S, Chen Y L, Goennenwein S T B and Felser C 2018 *Nat. Phys.* **14** 1125
[17] Ye L D, Kang M G, Liu J W, Von Cube F, Wicker C R, Suzuki T, Jozwiak C, Bostwick A, Rotenberg E, Bell D C, Fu L, Comin R and Checkelsky J G 2018 *Nature* **555** 638
[18] Yin Q W, Tu Z J, Gong C S, Fu Y, Yan S H and Lei H C 2021 *Chin. Phys. Lett.* **38** 037403
[19] Chen K Y, Wang N N, Yin Q W, Gu Y H, Jiang K, Tu Z J, Gong C S, Uwatoko Y, Sun J P, Lei H C, Hu J P and Cheng J G 2021 *Phys. Rev. Lett.* **126** 247001
[20] Nie L P, Sun K L, Ma W R, Song D W, Zheng L X, Liang Z W, Wu P, Yu F H, Li J, Shan M, Zhao D, Li S J, Kang B L, Wu Z M, Zhou Y B, Liu K, Xiang Z J, Ying J J, Wang Z Y, Wu T and Chen X H 2022 *Nature* **604** 59
[21] Feng X L, Jiang K, Wang Z Q and Hu J P 2021 *Sci. Bull.* **66** 1384
[22] Ni S L, Ma S, Zhang Y H, Yuan J, Yang H T, Lu Z Y W, Wang N N, Sun J P, Zhao Z, Li D, Liu S B, Zhang H, Chen H, Jin K, Cheng J G, Yu L, Zhou F, Dong X L, Hu J P, Gao H J and Zhao Z X 2021 *Chin. Phys. Lett.* **38** 057403
[23] Mielke A 1992 *J. Phys. A: Math. Gen.* **25** 4335
[24] Kiesel M L, Platt C and Thomale R 2013 *Phys. Rev. Lett.* **110** 126405
[25] Imada M and Kohno M 2000 *Phys. Rev. Lett.* **84** 143
[26] Miyahara S, Kusuta S and Furukawa N 2007 *Physica C* **460–462** 1145
[27] Tang E, Mei J W and Wen X G 2011 *Phys. Rev. Lett.* **106** 236802
[28] Mielke A 1991 *J. Phys. A* **24** 3311
[29] Tasaki H 1998 *Rep. Prog. Phys.* **99** 489
[30] Cao Y, Fatemi V, Demir A, Fang S A, Tomarken S L, Luo J Y, Sanchez-Yamagishi J D, Watanabe K, Taniguchi T, Kaxiras E, Ashoori R C and Jarillo-Herrero P 2018 *Nature* **556** 80
[31] Cao Y, Fatemi V, Fang S A, Watanabe K, Taniguchi T, Kaxiras E and Jarillo-Herrero P 2018 *Nature* **556** 43
[32] Li Z, Zhuang J, Wang L, Feng H, Gao Q, Xu X, Hao W, Wang X, Zhang C, Wu K, Dou S X, Chen L, Hu Z and Du Y 2018 *Sci. Adv.* **4** eaau4511
[33] Wang L, Shih E M, Ghiotto A, Xian L D, Rhodes D A, Tan C, Claassen M, Kennes D M, Bai Y S, Kim B H, Watanabe K, Taniguchi T, Zhu X Y, Hone J, Rubio A, Pasupathy A N and Dean C R 2020 *Nat. Mater.* **19** 861
[34] Zi H, Zhao L X, Hou X Y, Shan L, Ren Z A, Chen G F and Ren C 2020 *Chin. Phys. Lett.* **37** 097403
[35] Chen X, Zhan X H, Wang X J, Deng J, Liu X B, Chen X, Guo J G and Chen X L 2021 *Chin. Phys. Lett.* **38** 057402
[36] Meier W R, Du M H, Okamoto S, Mohanta N, May A F, McGuire M A, Bridges C A, Samolyuk G D and Sales B C 2020 *Phys. Rev. B* **102** 075148
[37] Thouless D J 1977 *Phys. Rev. Lett.* **39** 1167
[38] Bither T A, Donohue P C and Young H S 1971 *J. Solid State Chem.* **3** 300
[39] Tsigankov D N and Efros A L 2002 *Phys. Rev. Lett.* **88** 176602
[40] Ovadyahu Z and Imry Y 1985 *J. Phys. Chem. C* **18** L19
[41] Rosenbaum R, Heines A, Karpovski M, Pilosof M and Witcomb M 1997 *J. Phys. Condens. Matter* **9** 5413
[42] Zhou Y, He X Y, Wang S Y, Wang J, Chen X L, Zhou Y H, An C, Zhang M, Zhang Z T and Yang Z R 2022 arXiv:2203.16943 [cond-mat.supr-con]
[43] Wang Q, Qiu X L, Pei C Y, Gong B C, Gao L L, Zhao Y, Cao W Z, Li C H, Zhu S H, Zhang M X, Chen Y L, Liu K and Qi Y P 2022 arXiv:2204.05179 [cond-mat.supr-con]
[44] Perez-Gonzalez A 1996 *Phys. Rev. B* **54** 16053
[45] Fulde P 1973 *Adv. Phys.* **22** 667
[46] Nakamura D, Adachi T, Omori K, Koike Y and Takeyama S 2019 *Sci. Rep.* **9** 16949
[47] Yuan H Q, Singleton J, Balakirev F F, Baily S A, Chen G F, Luo J L and Wang N L 2009 *Nature* **457** 565
[48] Ashcroft N W and Mermin N D 1976 *Solid State Physics* (Philadephia: Saunders College Publishing) p 240
[49] Li P C, Balakirev F F and Greene R L 2007 *Phys. Rev. Lett.* **99** 047003
[50] Hwang H Y, Batlogg B, Takagi H, Kao H L, Kwo J, Cava R J, Krajewski J J and Peck W F 1994 *Phys. Rev. Lett.* **72** 2636